

The microstructure–mechanical properties relationships of BaTiO₃

W.H. Tuan*, S.K. Lin

Institute of Materials Science & Engineering, National Taiwan University, Taipei, Taiwan

Received 9 May 1997; accepted 27 September 1997

Abstract

Barium titanate (BaTiO₃) specimens are sintered under different conditions to produce different microstructures. These microstructures are composed of fine grains or duplex grains or coarse (abnormal) grains. The mechanical properties are determined as a function of microstructure. Microcracks are generated together with the formation of abnormal grains. The presence of microcracks enhances the toughness of BaTiO₃. The fracture of duplex-grained specimens originates from abnormal grains. The Weibull modulus of duplex-grained specimens is high for the size distribution of abnormal grains is narrow. There are only abnormal grains in the coarse-grained specimens. Microcracks are connected with one another in the specimens. The strength of the coarse-grained specimens is thus low. © 1998 Elsevier Science Limited and Techna S.r.l. All rights reserved

1. Introduction

Barium titanate (BaTiO₃) is widely used as a dielectric material for its high dielectric constant. However, in order to use the materials for electronic components, not only the dielectric properties but also the mechanical properties are important. For examples, a stress of 30–50 MPa is generated in the capacitor during end termination and soldering [1]. However, the mechanical properties of BaTiO₃ have attracted less attention. In a recent review made by G. de With [1], the reported values of the mechanical properties for BaTiO₃ are summarised. The reported values are scattered dramatically. The scatter may result from different materials, microstructures and measuring techniques. The mechanical properties depend strongly on the microstructure [2,3]. The relationships between the microstructure and mechanical properties of BaTiO₃ are investigated in the present study.

2. Experimental

A BaTiO₃ powder (No. 219-6, Ferro Co., USA) having Ba/Ti ratio of 0.995 was used in the present study. The powder was dispersed in de-ionized water. From a preliminary study, PAA-N (ammonium salt of polyacrylic

acid, Aldrich Chem. Co., USA) could be used as the dispersing agent to disperse the BaTiO₃ powder in water. The amount of the dispersing agent used was 0.175 wt% relative to BaTiO₃. The slurry was milled for 4 h with a turbo-mixer. The grinding medium used was zirconia balls. The slurry was then pressure filtered with a stainless mold to remove the water. The pressure applied was 1 MPa. The cake was then dried in an oven at 40°C for 3 days, at 60°C for 1 day and at 105°C for 1 day. The green compact was ground with SiC paper to remove 0.15 mm from the top and bottom surfaces. This procedure was adopted to avoid contamination. The size of the resulting green compact was 60 mm in diameter and 5.2 mm in thickness. The pore structure in the green compact was determined by a mercury porosimetry (Autopore II 9220, Micromeritics Instrument Co., USA).

The green compacts were heated at 3°C min⁻¹ to 600°C for 30 min to remove the dispersing agent. The compacts were then heated to the sintering temperature. Four temperature/time profiles, (1) 1290°C/7.5 min, (2) 1290°C/120 min, (3) 1290°C/600 min and (4) 1330°C/120 min were used to sinter the compacts. The heating and cooling rates were 3°C min⁻¹. The discs were then cut with diamond blade into rectangular bars. The bars were ground longitudinally with a 325 grit diamond wheel at a cutting depth of 5 mm per pass. The final dimensions of the specimens were 3×4×36 mm. The specimens were then chamfered with 200 grit SiC papers. The strength of the specimens was determined

* Corresponding author.

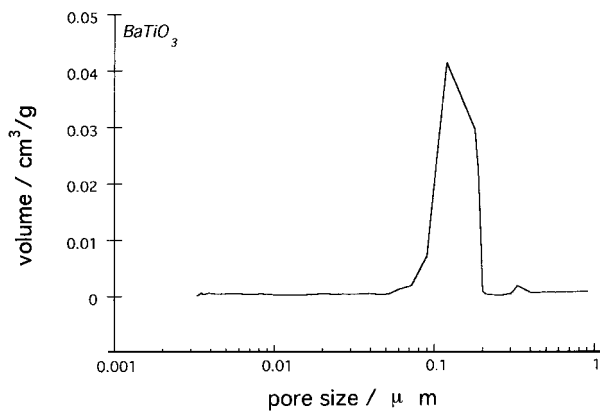


Fig. 1. The pore size distribution for the green compact.

by the four-point bending technique. The upper and lower spans were 10 and 30 mm, respectively. The fracture toughness was determined by the single-edge notched beam (SENB) technique. The notch was generated by cutting with a diamond saw. The thermal expansion curve of the fired specimens was determined with a dilatometer (Theta Co., USA). The heating and cooling rates were $3^{\circ}\text{C min}^{-1}$. The specimens were heated to 300°C and held at temperature for 1 h. The linear expansion curves of the specimens during heating, dwell, and cooling were recorded.

The final density was determined by a water displacement method. The polished surfaces were prepared by grinding with SiC papers and by polishing with alumina particles. The polished surface was chemically etched with a HCl-HF solution to reveal the grain boundaries. The microstructure was observed with optical microscopy (OM) or scanning electron microscopy (SEM). The area fraction of abnormal grains was determined by using an image analyzer (Quantimet 520, Cambridge Co., UK). The size of BaTiO_3 grains was determined with the linear intercept technique.

3. Results and discussion

The pore structure of the green compact is shown in Fig. 1. The pores are distributed in a rather narrow range, 0.1 μm to 0.2 μm . The green structure is uniform. The pressure infiltration technique used in the present study can produce a uniform green structure. The density and grain size of the fired specimens are shown in Table 1. The relative density of the specimens varies from 94.0 to 98.5%. The microstructures of the specimens are shown in Fig. 2. There are no abnormal grains observed in the specimens sintered at 1290°C for 7.5 min. The specimens sintered at 1290°C for 7.5 min are termed as fine-grained specimens. For specimens sintered at 1290°C for 120 and 600 min, there are 18 and 49 vol %, respectively, of abnormal grains present. The microstructure is duplex in nature. The specimens are termed as duplex-grained specimens. The size of the abnormal grains ranges from 30 to 40 μm . For the specimens sintered at 1330°C for 120 min, the grain size is 37 μm . From microstructural observation, (Fig. 2), the abnormal grains start to form at 1290°C for longer than 7.5 min. Some fine grains are consumed to form abnormal grains. As the specimens are sintered at 1330°C for 120 min, all the fine grains are consumed by abnormal grains.

The Weibull curves for the specimens sintered with different sintering profiles are shown in Fig. 3. The average strength of the specimens is shown in Table 1. For the specimens sintered at 1290°C , the strength of the specimens sintered for 7.5 min is the lowest. The strength of brittle ceramics is very sensitive to the presence of porosity [4]. For barium titanate, the strength is decreased exponentially with the increase of porosity [5]. The strength of the fine-grained specimens is low for their relatively low density. The average strength and Weibull modulus are the same for the specimens sintered at 1290°C for 120 and 600 min. As the specimens are sintered at 1330°C , the strength is the lowest among

Table 1
The density, grain size, mechanical properties and dielectric properties of the sintered BaTiO_3

Sintering conditions	Fine-grained	Duplex-grained	Duplex-grained	Coarse-grained
	1290°C , 7.5 min	1290°C , 120 min	1290°C , 600 min	1330°C , 120 min
Relative density (%)	94.0	97.5	98.5	97.4
Amount of abnormal grains (vol %)	0	18	49	100
Size of abnormal grains (μm)	—	32	40	37
Size of fine grains (μm)	1.3	1.5	1.7	—
Average strength (MPa)	72	82	80	65
Weibull modulus	9 (20 ^a)	15 (23 ^a)	18 (17 ^a)	13 (21 ^a)
Toughness ($\text{MPa m}^{0.5}$)	1.1	1.2	1.5	1.6
Flaw size (μm)	45	41	68	117
Dielectric constant	2760	2610	2250	1600
Dissipation factor	0.017	0.019	0.014	0.015

^a Number of specimens used to determine the Weibull modulus.

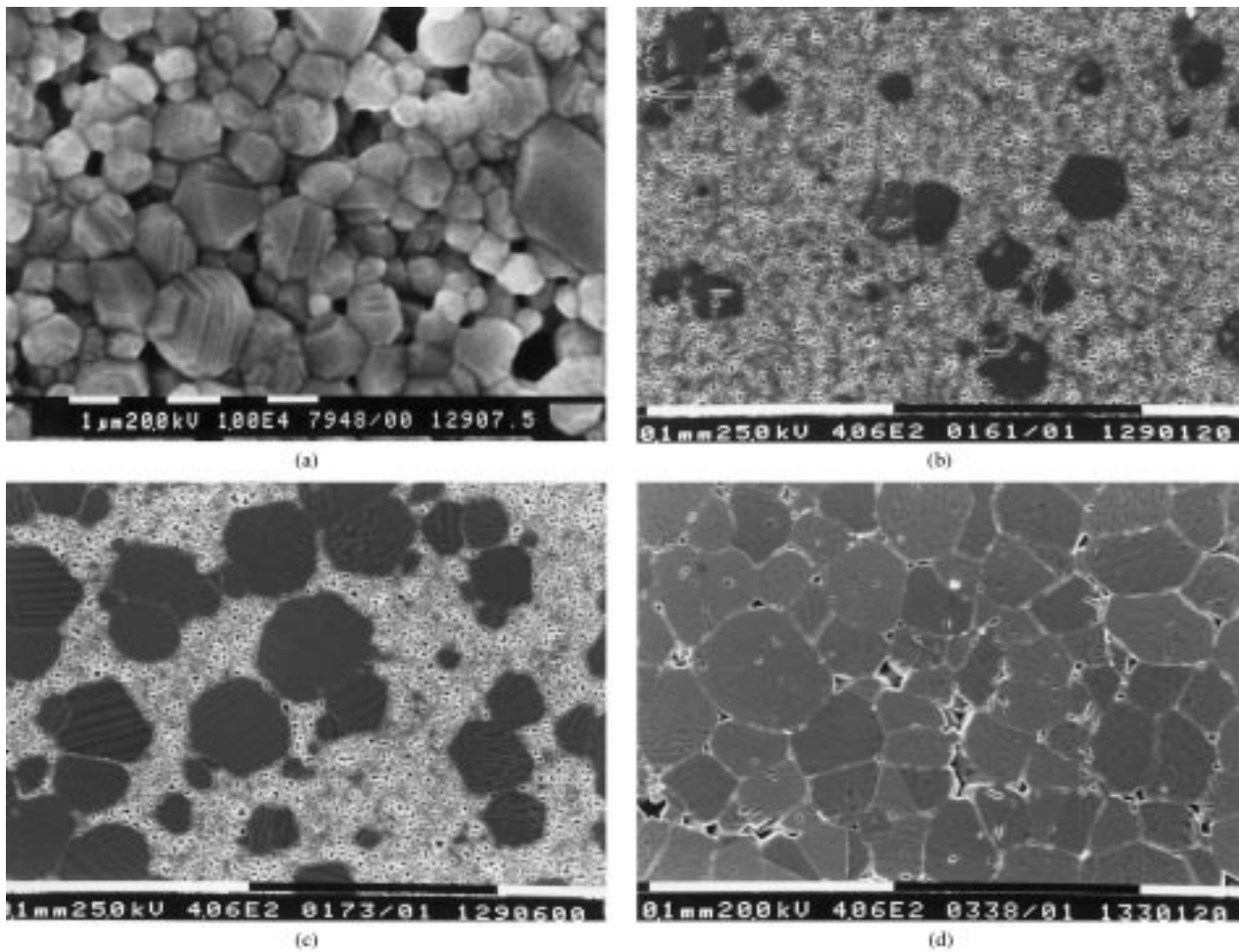


Fig. 2. The microstructure of the sintered specimens. The specimens are sintered at 1290°C for (a) 7.5 min (b) 120 min (c) 600 min and (d) at 1330°C for 120 min.

all the specimens. It results from their coarse microstructure. The fracture toughness of the specimens is shown as a function of the amount of coarse grains in Fig. 4. The toughness increases with increasing amount of coarse grains.

Ceramics are known to fracture in a brittle, Griffith fashion. The size of critical flaw, C , can be estimated by using Griffith equation as

$$\sqrt{C} = \frac{K_{IC}}{\sigma Y} \quad (1)$$

In the equation, K_{IC} is the fracture toughness, σ the strength and Y a geometrical constant. The calculated size of critical flaw is shown in Table 1. There are no abnormal grains in the fine-grained specimens. The size of critical flaw is much larger than the average grain size. It indicates that fracture is dominated by processing flaws. The formation of processing flaws can relate to the powder characteristics and processing techniques

[6]. The value of the Weibull modulus reflects the size distribution of the processing flaws.

As specimens are sintered at 1290°C for 120 and 600 min, both fine and coarse grains are existed. A typical fracture surface for duplex-grained specimens is shown in Fig. 5. The specimen is sintered at 1290°C for 120 min. The fracture originates from an abnormal grain. It indicates that the abnormal grains act as fracture origin. The size of abnormal grains is similar to the size of processing flaws (Table 1). It further confirms that fracture is originated from abnormal grains. The fracture is then dominated by the abnormal grains instead of the pre-existed processing flaws. The formation of nuclei for abnormal grains is suggested to originate from heterogeneity in chemical composition and particle size [7,8]. Such heterogeneities commonly occur in commercial BaTiO_3 powders. The heterogeneities may distribute randomly in the compact. The nuclei of abnormal grains are thus distributed randomly within the structure. The size of abnormal grains depends strongly on the composition and sintering

temperature [7]. In the present study, the sintering temperatures were varied over a very narrow range. The final size of abnormal grains is thus similar for the specimens prepared in the present study (Table 1). It may also imply that the size distribution of abnormal grains is uniform. Since the fracture originates from abnormal grains, the scatter of the strength value is narrow. The Weibull modulus is therefore high for the duplex-grained microstructure. Furthermore, the Weibull modulus is similar for the specimens containing different amount of abnormal grains.

In the specimens sintered at 1330°C, only coarse grains can be observed. As shown later, the formation of abnormal grains is accompanied with the formation of microcracks. If the number of microcracks is large enough, the microcracks can link to one another. The size of critical flaw is three times that of the grains in the coarse-grained specimens (Table 1). It suggests that microcrack of one abnormal grain links to other microcracks of adjacent abnormal grains. Several connected microcracks dominate the fracture behaviour. The size of connected microcracks varies from specimen to

specimen. The size of critical flaws also varies from specimen to specimen. The Weibull modulus is thus low.

The thermal expansion curves for the fine-grained, duplex-grained and coarse-grained specimens are shown in Fig. 6. For the fine-grained specimens, the expansion curve is very close to that of shrinkage curve. The volume changes associated with the phase transformation between tetragonal and cubic can be noted on the curve. For the duplex-grained specimens, the expansion and shrinkage curves are not matched well to each other, i.e. a hysteresis is observed. The separation between the expansion and shrinkage curves is the biggest in the expansion curve as the transformation taking place. For the coarse-grained specimens, the separation between the expansion and shrinkage is bigger than that of the duplex-grained specimens. The presence of expansion hysteresis can be related to the presence of grain boundary microcracks [9–11]. The presence of microcracks along grain boundaries provides a “cushion” into which adjacent grains may expand [11]. The hysteresis is thus formed as the specimen is heated and subsequently cooled. The volume change associated

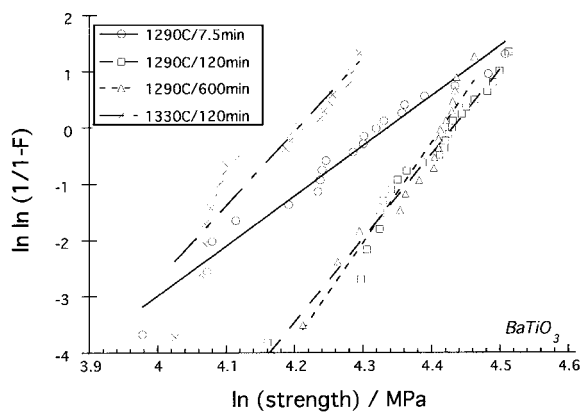


Fig. 3. The Weibull curves for the sintered specimens.

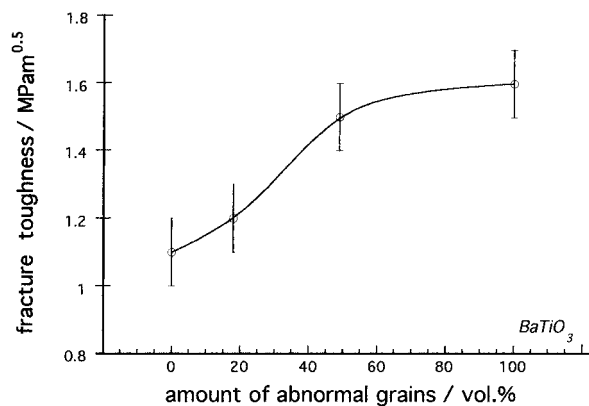
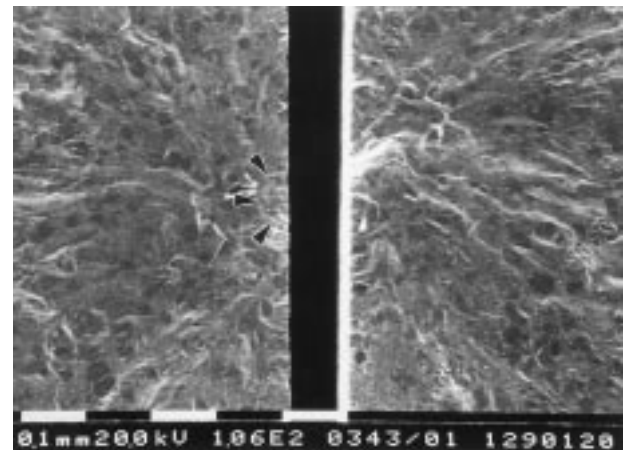
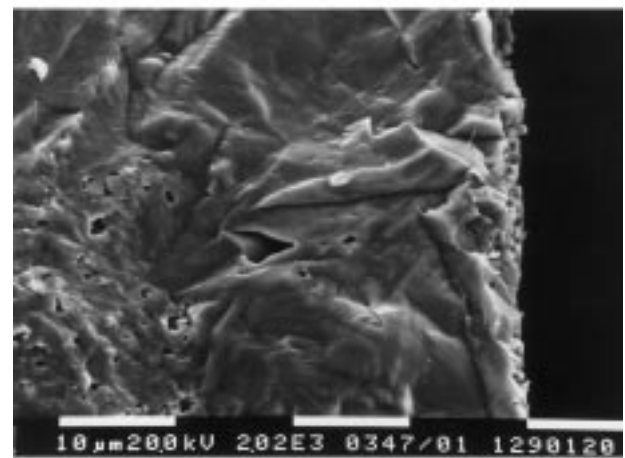


Fig. 4. The fracture toughness as a function of the amount of abnormal grains.



(a)



(b)

Fig. 5. (a) The fracture surface of a specimen with duplex microstructure. The fracture origin of the specimen is shown in (b).

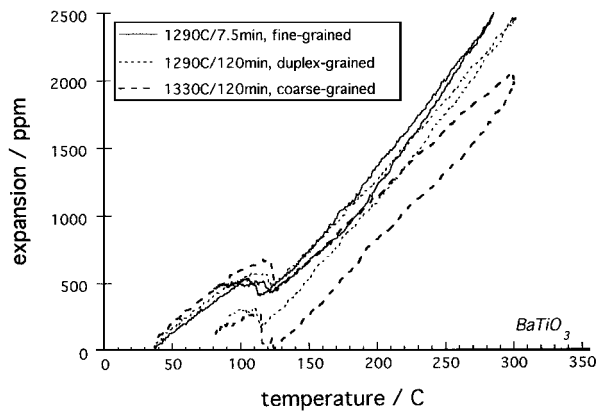


Fig. 6. The thermal expansion curves for the sintered specimens.

with the phase transformation occurs within a relatively short time. The matching between the expansion and shrinkage is more difficult. Furthermore, the phase below the Curie temperature is anisotropic in nature. The thermal expansion coefficient is different along different crystal orientations. The separation between the expansion and shrinkage at the phase transformation temperature is thus large. The hysteresis area of the coarse-grained specimens is larger than that of the duplex-grained specimens. It indicates that the microcrack density of the coarse-grained specimens is higher than that in the duplex-grained specimens.

Microcracks are frequently found together with the formation of abnormal grains. It results from the thermal expansion mismatch along different crystal orientation [11]. One example is shown in Fig. 7. The microcrack density is proportional to the amount of coarse grains. The presence of microcracks can enhance the fracture toughness [12]. The toughness is thus enhanced with increasing amount of coarse grains (Fig. 4). In the coarse-grained specimens, the coarse grains are near to one another. The microcracks can

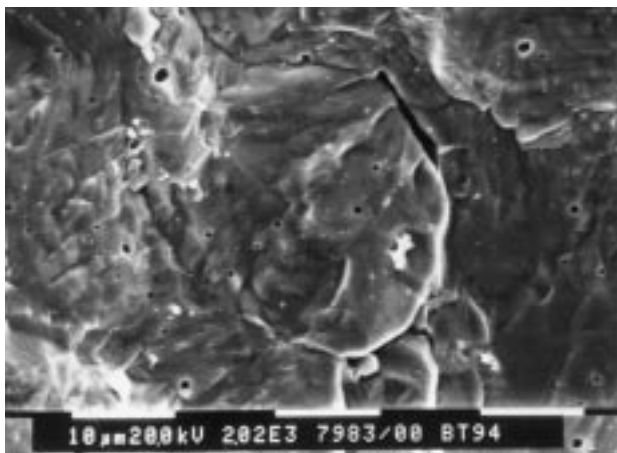


Fig. 7. A microcrack observed at the grain boundary of coarse grains.

link to one another. The strength is thus decreased [13] (Table 1).

The dielectric constant and dissipation factor at room temperature are shown in Table 1. Previous studies indicate that the dielectric constant depends strongly on microstructure. [14,15] This is also demonstrated in Table 1. The dielectric constant decreases with the increasing amount of coarse grains. The dissipation factor for all the specimens is less than 2%. The factor shows little dependence on microstructure.

4. Conclusions

The relationships between microstructure and mechanical properties of BaTiO_3 are investigated. The green compacts are prepared by a pressure infiltration technique. Uniform green structure results from this technique. The green compacts are sintered with different sintering conditions. As sintering time is prolonged or sintering temperature is raised, abnormal grains are formed. The formation of abnormal grains leads to the formation of microcracks. The presence of microcracks is verified by investigating the thermal expansion behaviour. Due to the presence of microcracks, the fracture is originating from the abnormal grains. The size of abnormal grains shows little dependence on the sintering conditions used in the present study. Due to the narrow size distribution of abnormal grains, the Weibull modulus for the duplex-grained specimens is high. The presence of microcracks can also enhance the fracture toughness. However, as the number of microcracks is high enough for microcracks to connect to one another, the strength is reduced.

References

- [1] G. de With, Structural integrity of ceramic multilayer capacitor materials and ceramic multilayer capacitors, *J. European Ceram. Soc.* 12 (1993) 323–336.
- [2] W.H. Tuan, M.J. Lai, M.C. Lin, C.C. Chan, S.C. Chiu, The mechanical performance of alumina as a function of grain size, *Mater. Chem. & Phys.* 36 (1994) 246–251.
- [3] T. Watari, H. Hyakutake, T. Torikai, O. Matsuda, M. Endo, T. Motone, Mechanical properties of strontium ferrites with duplex structure, *Ceramics International* 21 (1995) 89–95.
- [4] F.P. Kundsen, Dependence of mechanical strength of brittle polycrystalline specimens on porosity and grain size, *J. Am. Ceram. Soc.* 42 (1959) 376–80.
- [5] R.C. Pohanka, R.W. Rice, B.E. Walker Jr, Effect of internal stress on the strength of BaTiO_3 , *J. Am. Ceram. Soc.* 59 (1976) 71–76.
- [6] F.F. Lange, Powder processing science and technology for increased reliability, *J. Am. Ceram. Soc.* 72 (1989) 3–15.
- [7] D. Kolar, Discontinuous grain growth in multiphase ceramics, *Ceramic Transactions* 7 (1988) 529–545.
- [8] C.-H. Lu, W.H. Tuan, B.-K. Fang, Effect of pre-sintering heat treatment on the microstructure of barium titanate, *J. Mater. Sci. Letters* 15 (1996) 43–45.

- [9] W.R. Manning, O. Hunter Jr, F.W. Calderwood, D.W. Stacy, Thermal expansion of Nb_2O_5 , *J. Am. Ceram. Soc.* 55 (1972) 342–347.
- [10] J.A. Kuszyk, R.C. Bradt, Influence of grain size on effects of thermal expansion anisotropy in MgTi_2O_5 , *J. Am. Ceram. Soc.* 56 (1973) 420–423.
- [11] F.J. Parker, R.W. Rice, Correlation between grain size and thermal expansion for aluminum titanate materials, *J. Am. Ceram. Soc.* 72 (1989) 2364–2366.
- [12] A.G. Evans, K.T. Faber, Toughening of ceramics by circumferential microcracking, *J. Am. Ceram. Soc.* 64 (1981) 394–398.
- [13] N. Claussen, J. Steeb, R.F. Pabst, Effect of induced microcracking on the fracture toughness of ceramics, *Am. Ceram. Soc. Bull.* 56 (1977) 559–562.
- [14] K. Kinoshita, A. Yamaji, Grain-size effects on dielectric properties in barium titanate ceramics, *J. Appl. Phys.* 47 (1976) 371–373.
- [15] T.T. Fang, H.L. Hsieh, F.S. Shiau, Effects of pore morphology and grain size on the dielectric and tetragonal-cubic phase transition of high-purity barium titanate, *J. Am. Ceram. Soc.* 76 (1993) 1205–1211.